MEDICAL RADIOLOGY

Diagnostic Imaging

Editors:
A. L. Baert, Leuven
M. Knauth, Göttingen

A. M. Davies · M. Sundaram · S. L. J. James
(Eds.)

Imaging of Bone Tumors and Tumor-Like Lesions

Techniques and Applications

With Contributions by

S. Anderson-Sembach · L. W. Bancroft · J. L. Bloem · M. A. Bredella · P. Brys
R. S. D. Campbell · V. N. Cassar-Pullicino · P. Choong · A. Davies · A. M. Davies
A. M. de Schepper · R. Erlemann · A. Gogna · R. A. R. Green · D. Hobin · A. J. Huang
S. Hwang · H. Ilaslan · S. L. J. James · Karl J. Johnson · G. Jundt · A. W. Kao
S. V. Kattapuram · L. G. Kindblom · M. Koplas · N. A. Kotnis · M. J. Kransdorf
R. K. Lalam · K. Ludwig · N. M. Major · D. Malfair · D. C. Mangham · S. Mannava
P. L. Munk · M. D. Murphey · P. G. O'Donnell · D. M. Panicek · K. M. Patel · B. Peersman
W. C. G. Peh · Etienne Pluot · V. N. Cassar-Pullicino · D. Ritchie · A. Saifuddin
D. Sanghvi · C. Simpfendorfer · J. A. Skinner · A. S. Suhardja · M. Sundaram · B. J. Tins
P. N. M. Tyrrell · F. M. Vanhoenacker · F. van Kerkhove · S. Verbeke · K. Verstraete
R. W. Whitehouse · M. H. Willis

Foreword by
A. L. Baert

Springer

A. Mark Davies, MBCHB, FRCR
Consultant Radiologist
MRI Department
Royal Orthopaedic Hospital NHS Foundation Trust
Bristol Road South
Northfield
Birmingham B31 2AP
UK

Steven J. James, MD
Consultant Radiologist
Imaging Department
Royal Orthopaedic Hospital NHS Foundation Trust
Bristol Road South
Northfield
Birmingham B31 2AP
UK

Murali Sundaram, MD
Section of Musculoskeletal Radiology, Imaging Institute, Cleveland Clinic
Professor of Radiology, Cleveland Clinic Lerner School of Medicine
of Case Western Reserve University
Diagnostic Radiology/A21
The Cleveland Clinic Foundation
9500 Euclid Avenue
Cleveland, OH 44195
USA

Medical Radiology · Diagnostic Imaging and Radiation Oncology
Series Editors:
A.L. Baert · L.W. Brady · H.-P. Heilmann · M. Knauth · M. Molls · C. Nieder

Continuation of Handbuch der medizinischen Radiologie
Encyclopedia of Medical Radiology

ISBN 978-3-540-77982-7 e-ISBN 978-3-540-77984-1

DOI 10.1007/978-3-540-77984-1

Library of Congress Control Number: 2008 9307 83

Cover design: Verlagsservice Teichmann, Mauer, Germany
Production, reproduction and typesetting: le-tex publishing services GmbH, Leipzig, Germany

Printed on acid-free paper

9 8 7 6 5 4 3 2 1

springer.com

Foreword

Detection and characterization of bone tumors with imaging remains a big challenge for every radiologist notwithstanding the impressive progress achieved by the introduction of several new imaging modalities. Moreover, new concepts in surgical and oncological treatment of these lesions require from the radiologist appropriate and focused answers to the specific questions asked by the referring physicians in order to choose the best therapeutic approach for the individual patient.

This comprehensive textbook describes in detail the possibilities and limits of all modalities, including MRI, CT, nuclear medicine and interventional radiological procedures, employed for the modern imaging of tumoral and tumor-like lesions of bone. Their role in the diagnosis, surgical staging, biopsy and assessment of response to therapy is discussed in detail, covering all tumor subtypes as well as their specific anatomical location.Well selected and technically impeccable illustrations strongly enhance the didactic value of this work.

I am very much indebted and grateful to the three editors: A. Mark Davies, Murali Sundaram and Steven L. J. James, world authorities in musculoskeletal radiology, for their superb scientific achievement in preparing and editing this wonderful volume as well as for their individual chapters. I would also like to thank the large international group of collaborating authors, who are also widely acknowledged for their specific expertise in the area of bone tumors, for their outstanding contributions.

I am convinced that this unique book will be of great help to certified radiologists and radiologists in training to assist them in their daily clinical duties. However, orthopedic surgeons and oncologists also will find it extremely helpful to guide them in the therapeutic management of their patients.

I have no doubt that it will meet great success with the readership of this book series.

Leuven

Albert L. Baert
Series Editor

Preface

As our understanding of the complex subject of bone tumours improves, there is a need for the continuous updating of radiologists, orthopaedic surgeons, oncologists and other professionals working in this area. This book takes a multifaceted approach to the subject.

After an initial introductory chapter covering classification and epidemiology the first section acquaints the reader with the range of techniques available for imaging bone tumours. These five chapters cover magnetic resonance imaging, computed tomography, ultrasound, interventional techniques and nuclear medicine. The expanding role of PET scanning is included in this last chapter. The next six chapters apply these techniques to the general diagnosis and management of bone tumours including image-guided biopsy techniques, surgical staging and assessment of tumour response to different treatments. The third and largest section comprises 18 chapters detailing the salient clinical and imaging features of all the important tumour subtypes (cartilaginous, osteogenic etc.). The fourth section reviews the types of tumours that may be found at particular anatomical sites such as the ribs, scapula, spine and so on. Finally there is a chapter covering the important topic of compartmental anatomy and a further chapter giving potted biographies of those whose names over the past 150 years have become synonymous with bone tumours.

The editors are grateful to the international panel of authors for their contributions to this book, which aims to provide a comprehensive overview of current imaging of tumours and tumour-like lesions of bone.

Birmingham, UK — A. Mark Davies
Cleveland, US — Murali Sundaram
Birmingham, UK — Steven L. J. James

Contents

1 **Bone Tumors: Epidemiology, Classification, Pathology** 1
Lars Gunnar Kindblom

2 **Computed Tomography of Bone Tumours** 17
Richard W. Whitehouse

3 **Imaging Techniques: Magnetic Resonance Imaging** 31
Sinchun Hwang and David M. Panicek

4 **Nuclear Medicine** 53
Ruth A. R. Green

5 **Ultrasonography** 85
Alun Davies and Asif Saifuddin

6 **Interventional Techniques** 95
Steven L. J. James

7 **Principles of Detection and Diagnosis** 111
A. Mark Davies and Victor N. Cassar-Pullicino

8 **Biopsy** 139
Apoorva Gogna, Wilfred C. G. Peh and Peter L. Munk

9 **Surgical Staging 1: Primary Tumour** 163
Alun Davies, John Skinner and Asif Saifuddin

10 **Surgical Staging 2: Metastatic Disease** 183
Ambrose J. huang, Marc H. Willis, Susan V. Kattapuram and Miriam A. Bredella

11 **Assessment of Response to Chemotherapy and Radiotherapy** 199
Koenraad Verstraete

12 Assessment of Locally Recurrent Disease 211
Marc H. Willis, Ambrose J. Huang, Miriam A. Bredella and Susan V. Kattapuram

13 Cartilage Tumours 225
Karl Ludwig

14 Osseous Tumors 251
Mark J. Kransdorf and Mark D. Murphey

15 Fibrogenic and Fibrohistiocytic Tumors 307
Monica Koplas and Murali Sundaram

16 Giant Cell Tumor 321
Mark J. Kransdorf and Mark D. Murphey

17 Ewing Sarcoma/PNET Tumors 337
Filip M. Vanhoenacker, Filip van Kerkhove, Benjamin Peersman, Peter Brys and Arthur M. de Schepper

18 Hematopoietic Tumors 351
Laura W. Bancroft

19 Angiomatous Neoplasms of the Skeletal System 365
Agustinus S. Suhardja, Sophie Verbeke and Johan L. Bloem

20 Notochordal Tumours 375
V. N. Cassar-Pullicino and D. C. Mangham

21 Smooth Muscle Tumors 393
Claus Simpfendorfer and Murali Sundaram

22 Lipogenic Tumours of Bone 401
Robert S. D. Campbell

23 Fibrous Dysplasia, Osteofibrous Dysplasia, and Adamantinoma 411
Sriram Mannava and Murali Sundaram

24 Cystic Lesions of Bone 425
Paul G. O'Donnell

25 **Langerhans Cell Histiocytosis** 447
Karl Johnson and David Hobin

26 **Bone Metastases 1: Spine** 461
Prudencia N. M. Tyrrell, Victor N. Cassar-Pullicino, Radhesh K. Lalam and Bernhard J. Tins

27 **Bone Metastases 2: Pelvis and Appendicular Skeleton** 481
Bernhard J. Tins, Radhesh K. Lalam, Victor M. Cassar-Pullicino and Prudencia N. M. Tyrrell

28 **Radiation-Induced Tumours** 503
A. Mark Davies and Steven L. J. James

29 **Tumour and Tumour-like Conditions Associated with Paget's Disease of Bone** 515
A. Mark Davies, Etienne Pluot and Steven L. J. James

30 **Reactive, Metabolic, and Tumor-Like Lesions of Bone** 531
Darshana Sanghvi and Murali Sundaram

31 **Tumours of the Ribs and Clavicle** 553
David Malfair and Peter L. Munk

32 **Scapula** 563
Suzanne E. Anderson-Sembach, Rainer Erlemann, Peter Choong and Gernot Jundt

33 **Anatomical Considerations: Spine and Sacrum** 587
Amy W. Kao and Hakan Ilaslan

34 **Bony Pelvis** 603
David Ritchie

35 **Hand and Wrist** 621
Nikhil A. Kotnis, A. Mark Davies and Steven L. J. James

36 **Tumours and Tumour-Like Lesions of the Patella** 637
Etienne Pluot, A. Mark Davies and Steven L. J. James

37 **Tumours of the Foot** 647
David A. Ritchie

38 Compartmental Anatomy 665
Kavita M. Patel and Nancy M. Major

39 Who Was Who in Bone Tumours 677
Etienne Pluot, A. Mark Davies and Steven L. J. James

Subject Index 687

List of Contributors 693

Bone Tumors: Epidemiology, Classification, Pathology

1

Lars Gunnar Kindblom

CONTENTS

1.1 **Introduction** *2*

1.2 **Epidemiology** *2*

1.3 **Morphologic Diagnosis of Bone Tumors** *5*

1.4 **Types of Bone Tumor Specimens** *6*
1.4.1 Intraoperative Procedures/ Frozen Sections *6*
1.4.2 Fine-needle Aspiration Biopsy *6*
1.4.3 Biopsy *6*
1.4.4 Curettage *6*
1.4.5 Resections and Amputations *6*

1.5 **Adjunctive Diagnostic Techniques** *7*
1.5.1 Histochemistry, Immunohistochemistry, and Electron Microscopy *7*
1.5.2 Cytogenetic/Molecular Genetic Techniques *7*

1.6 **Classification of Bone Tumors** *7*

1.7 **Comments on the Morphologic Classification of Bone Tumors** *7*
1.7.1 Cartilage Tumors *7*
1.7.2 Bone-forming Tumors *9*
1.7.3 Ewing's Sarcoma and Other Small Round Cell Malignancies *9*
1.7.4 Giant Cell Tumors *9*
1.7.5 Fibrogenic/Fibrohistiocytic Tumors *9*
1.7.6 Chordoma *10*
1.7.7 Vascular Tumors *10*
1.7.8 Soft Tissue Tumor Types Occurring as Primary Bone Tumors *10*
1.7.9 Conditions Simulating Primary Bone Tumors *10*

1.8 **Congenital, Hereditary, and Non-hereditary Syndromes Associated with Bone Tumors** *14*

References *14*

KEY POINTS

- Primary bone tumors are rare; non-neoplastic conditions, metastatic disease, and lymphohematologic malignancies, which may simulate primary bone tumors, by far outnumber genuine bone tumors.
- Excluding myeloma and lymphoma, malignant primary bone tumors constitute only 0.2% of all malignancies in adults and approximately 5% of childhood malignancies.
- Bone tumor classification is based on morphologic findings: cell type, architecture, and matrix production. The morphologic features of benign and malignant as well as non-neoplastic conditions and true tumors may overlap.
- Many bone tumor entities show a striking consistency in clinical setting and age and anatomic site distribution.
- The final diagnosis of bone tumors should be based on a synthesis of histopathologic findings, clinical presentation, and imaging characteristics, preferably in the setting of a multidisciplinary team conference.
- Adjunctive immunohistochemical and genetic/molecular genetic techniques are important for the definite classification of certain bone tumors.
- A number of congenital, hereditary, and non-hereditary syndromes are associated with increased risk of bone tumors.

L.-G. Kindblom, MD, PhD
Professor of Pathology, Department of Musculoskeletal Pathology at the Royal Orthopaedic Hospital NHS Foundation Trust, Robert Aitken Institute for Clinical Research, The Medical School, University of Birmingham, Birmingham B15 2TT, UK

1.1 Introduction

Primary bone tumors are fairly rare. Conditions that may simulate primary bone tumors, such as metastasis and non-neoplastic conditions such as inflammatory processes, bone cysts, fibrous dysplasia, non-ossifying fibroma, Paget's disease of bone, etc., by far outnumber the cases of true bone tumors. Compared to other malignancies, primary malignant bone tumors are very rare. The three most common genuine primary bone malignancies (osteosarcoma, chondrosarcoma, and Ewing's sarcoma) account for only 0.2% of all malignancies in the UK and USA; however, in children (< 15 years) malignant bone tumors account for approximately 5% of all malignancies (Dorfman and Czerniak 1995, 1998; Unni et al. 2005). This chapter reviews the epidemiology and pathologic classification of bone tumors. In addition, it gives an overview of the pathologist's role in diagnosis and management.

1.2 Epidemiology

The vast majority of primary bone tumors are benign and since many are non-symptomatic they remain undetected or are detected only incidentally at radiographic examinations for other reasons. The true incidence of benign bone tumors has therefore been difficult to determine. The incidence of primary bone malignancies is, in contrast, fairly well documented in various national cancer registries. Excluding the most common lymphohematopoietic malignancies (particularly plasma cell tumor/myeloma and malignant lymphoma, more rarely leukemia) that are of bone marrow origin rather than true bone tumors, the yearly incidence in the USA has been estimated to be $8/10^6$. This corresponds well with the approximately 500 cases diagnosed yearly in the UK and some 2,500 cases in the USA. More than 75% of malignant bone tumors are osteosarcoma, chondrosarcoma, and Ewing's sarcoma (Table 1.1). The incidence of malignant bone tumors shows a striking age-specific distribution: in the age group 0–40 years, there is an incidence peak between 10 and 20 years (primarily osteosarcoma and Ewing's sarcoma) and for the age group above 40 years there is a steady increase in incidence up to 80 years (primarily chondrosarcoma and to a lesser degree Paget's related osteosarcoma) (Dorfman and Czerniak 1995, 1998; Unni et al. 2005).

Benign bone tumors and many bone simulating, non-neoplastic conditions also show a striking age distribution. This together with a likewise striking site distribution for both benign and malignant bone tumors is most helpful in the diagnosis of bone lesions. The combined information of age, site, and imaging findings can in reality in many instances indicate a definite diagnosis, sometimes to the point that morphologic confirmation is considered unnecessary (such as in cases of bone cysts, fibrous dysplasia, non-ossifying fibroma, Paget's disease of bone). For the pathologist, awareness of these age and site distributions is essential; when a suggested morphologic diagnosis occurs at a highly unusual site or in "the wrong" age group, the definite diagnosis should be carefully reevaluated. The age and anatomic site distributions of some of the most common bone tumors are summarized in Tables 1.2 and 1.3.

Table 1.1. Relative frequency of most common primary bone malignancies (excluding myeloma/malignant lymphoma) (Dorfman and Czerniak 1995)

Primary bone malignancy	Frequency (%)
Osteosarcoma	35.1
Chondrosarcoma	25.8
Ewing's sarcoma	16.0
Chordoma	8.4
Malignant fibrous histiocytoma	5.7
Angiosarcoma	1.4
Unspecified	1.2
Other	6.4

Table 1.2. Classification of primary benign bone tumors, peak age, and most common sites distribution

Histologic type	Peak age (years)	Most common sites	Comments
Cartilage tumors			
Osteochondroma	10–30	Distal femur, proximal tibia, proximal humerus, rarely from flat bones	> 2 cm cartilage cap may indicate malignant transformation
Enchondroma	10–40	Hands, feet, long tubular bones	
Periosteal chondroma	10–40	Proximal humerus, distal femur, hip region, and pelvis	Sharply demarcated from cortex
Chondroblastoma	10–30	Distal femur, proximal tibia and humerus, calcaneus	Typically epiphyseal
Chondromyxoid fibroma	10–30	Proximal tibia, distal femur, pelvis, feet (metatarsal)	
Osteogenic tumors			
Osteoid osteoma	5–25	Proximal femur, any long bones	Distinguished from osteoblastoma by size and imaging
Osteoblastoma	10–40	Spine, long tubular bones, jaws	
Fibrogenic tumors			
Desmoplastic fibroma	10–30	Mandible, femur, pelvis	Very rare; distinction from FD, low-grade osteosarcoma, and fibrosarcoma may be difficult
Fibrohistiocytic tumors			
Benign fibrous histiocytoma	20–60	Pelvis, femur	Diaphyseal or metaphyseal; rarely used concept, distinguished from non-ossifying fibroma only by clinical setting
Giant cell tumor	20–45	Distal femur, proximal tibia, distal radius, sacrum	Epiphyseal; pulmonary metastases occur in 2%; very rarely transformation to high-grade sarcoma
Vascular tumors			
Hemangioma (cavernous, capillary, epithelioid, etc.)	Classic hemangiomas, usually adults	Craniofacial bones, vertebrae	Hemangiomas are often multicentric
Angiomatosis, lymphangioma(tosis)	Often children	Highly variable	
Glomus tumor	Usually adults	Hands, distal phalanx	
Hemangiopericytoma	Usually adults	Pelvis	
Epithelioid hemangioendothelioma	Adults	Long tubular bones, spine	
Soft tissue type tumors			
Lipoma	Adults	Femur, calcaneus	All very rare
Schwannoma		Sacrum, mandible	
Leiomyoma		Mandible, tibia	

FD fibrous dysplasia

Table 1.3. Classification of primary malignant bone tumors, peak age, and most common sites distribution

Histologic type	Peak age (years)	Most common sites	Comments
Chondrosarcoma			
Primary	50–80	Pelvis, proximal/distal femur, proximal humerus, ribs	Usually large, intraosseous; very rarely periosteal
Secondary	20–60	Ex osteochondroma(tosis): pelvis, hip and shoulder	In Ollier's/Maffucci's at any site affected
Dedifferentiated chondrosarcoma	50–70	Pelvis, femur, humerus	Usually small component of low-grade chondrosarcoma juxtaposed with high-grade osteo-, spindle cell-, MFH-, or other sarcoma
Clear cell chondrosarcoma	25–60	Proximal femur, humerus	Typically epiphyseal location
Mesenchymal chondrosarcoma	10–40	Jaws, ribs, pelvis, spine	20–30% occur in soft tissues
Osteosarcoma			
Conventional	10–30	Distal femur, proximal tibia, hip and shoulder	Typically metaphyseal
Telangiectatic osteosarcoma	10–30	Femur, tibia, humerus	Typically metaphyseal; ABC-like, purely lytic
Low-grade central osteosarcoma	20–40	Distal femur, proximal tibia	May dedifferentiate to high grade
Parosteal osteosarcoma	20–50	Posterior distal femur, proximal humerus	May invade the bone, may dedifferentiate to high grade
Periosteal osteosarcoma	10–30	Femur, tibia	Diaphyseal, surface lesion, predominantly chondroblastic, intermediate grade
High-grade surface	10–40	Distal femur, shoulder	Diaphyseal or metaphyseal
Secondary osteosarcoma			
Paget's associated	50–90	Pelvis, hip and shoulder, craniofacial	High-grade osteosarcoma
Post-radiation	50–80	Pelvis, craniofacial, hip and shoulder, chest wall	High-grade osteosarcoma
Other conditions	40–70	Bones affected by FD, bone infracts, chronic osteomyelitis, etc.	
Ewing´s sarcoma, PNET	5–30	Pelvis, longbones of lower and upper extremities	
Fibrosarcoma, MFH, spindle cell sarcoma	40–70	Knee, hip and shoulder regions, pelvis	
Malignant giant cell tumor	20–60	Knee region, pelvis, shoulder region	High-grade sarcoma arising in GCT; classic GCT may rarely metastasize
Chordoma	30–80	Sacrococcygeal, skull base, vertebrae	May rarely dedifferentiate

ABC aneurysmal bone cyst, *FD* fibrous dysplasia, *GCT* giant cell tumor, *MFH* malignant fibrous histiocytoma, *PNET* primitive neuroectodermal tumor

Table 1.3. *(continued)* Classification of primary malignant bone tumors, peak age, and most common sites distribution

Histologic type	Peak age (years)	Most common sites	Comments
Angiosarcoma	20–70	Spine, pelvis, hip and shoulder regions	May be multicentric
Other soft tissue type sarcomas	20–70	Long bones, around major joints	Rare examples of leiomyosarcoma, liposarcoma, extraskeletal myxoid chondrosarcoma, synovial sarcoma, rhabdomyosarcoma, etc.
Adamantinoma	10–40	Tibia, rarely ulna, radius and fibula	Typically diaphyseal

ABC aneurysmal bone cyst, *FD* fibrous dysplasia, *GCT* giant cell tumor, *MFH* malignant fibrous histiocytoma, *PNET* primitive neuroectodermal tumor

1.3 Morphologic Diagnosis of Bone Tumors

The pathologic diagnosis of primary bone tumors poses particular problems:

1. Their rarity prevents most pathologists from gaining sufficient diagnostic experience.
2. There is an unusual need for the pathologist to be familiar with and to integrate clinical, laboratory, and imaging findings in the final diagnosis.
3. Despite their rarity, there is a wide spectrum of bone lesions with overlapping morphologic features.
4. The distinction between neoplastic, reactive/inflammatory, and metabolic bone lesions as well as some developmental disorders is sometimes difficult.
5. The diagnosis of malignant bone tumors, which frequently involve children or young adults, often has dramatic consequences in terms of surgical and adjuvant treatment. Moreover, there are a number of rare hereditary and non-hereditary conditions associated with increased risk of developing bone tumors that the pathologist needs to be aware of.

Even if clinical presentation and imaging studies are very often highly suggestive of a particular diagnosis, it is the morphologic findings that form the basis for the definite diagnosis of bone tumors. It is expected that the pathologists reporting primary bone malignancies participate in multidisciplinary team conferences and appropriately integrate clinical, laboratory, and imaging findings in the final diagnosis. Within these teams the pathologists have the important role to establish the correct diagnosis, to arrange for and interpret required adjunctive diagnostic tests (immunohistochemistry, cytogenetic/molecular analyses), to provide prognostic information, to identify patients that should be considered for adjuvant treatment protocols or trials, and to assess treatment response.

The possibility for the pathologist to correctly diagnose a bone tumor depends to a large extent on the completeness of the clinical and imaging information provided. The request forms for bone tumors should therefore contain information regarding pertinent clinical history, family history, laterality and exact anatomic site of tumor, whether the patient has solitary or multicentric disease or clinical evidence of metastatic disease, information on type and timing of any preoperative treatment, type of surgical procedure (fine-needle aspiration, core needle biopsy, open surgical biopsy, curettage, resection, amputation, etc.), and nature of specimen and, if indicated, orientation markers on specimen.

Whenever practically possible, it is advantageous if malignant bone tumor specimens are delivered fresh and unfixed to the pathology laboratory with the shortest possible delay. This will enable the pathologist to obtain material for studies that require fresh, unfixed tissue, to decide on the most appropriate way to obtain material from surgical margins, to decide on techniques for decalcification procedures, and to decide when dealing with large specimens if sectioning of skin, soft tissues, and bone is required to facilitate fixation.

1.4 Types of Bone Tumor Specimens

1.4.1 Intraoperative Procedures/ Frozen Sections

There are inherent problems with intraoperative diagnosis of bone tumors: hard, bony specimens cannot be processed since decalcification is needed, the pathologist needs to be familiar with the artifacts introduced by freezing specimens, and the overlapping morphologic features of different entities may be difficult to correctly interpret in frozen sections. However, where this technique is widely used, specialized bone tumor pathologists can acquire a very high degree of expertise. Frozen sections may be particularly helpful in determining if the biopsy is representative of the lesion and can help to immediately distinguish primary genuine bone tumors from inflammatory processes, other non-neoplastic conditions, metastases, and lymphohematologic malignancies.

1.4.2 Fine-needle Aspiration Biopsy

With the exception of Scandinavia, there are few bone tumor centers that have adopted this technique as a routine in the diagnosis of bone tumors. The reluctance to apply fine-needle aspiration biopsy (FNAB) is explained by the lack of experienced cytopathologists in this field, the limitations of the technique to obtain material from bony, calcified components, the loss of architecture and matrix characteristics, and the limited volume of tissue obtained (prohibiting extensive immunohistochemical and cytogenetic/molecular workup). In the hands of experienced cytopathologists, FNAB has, however, proven practically useful. For example, it is a very quick method to identify a lesion as a cartilage-producing neoplasm or hematologic malignancy (lymphoma/myeloma) and helps to distinguish osteosarcoma from Ewing's sarcoma and metastatic disease from primary bone tumors (Willen 1997). There are also reports of the diagnostic FNAB characteristics of many individual bone tumor entities such as osteosarcoma, chondrosarcoma, Ewing's sarcoma, and chordoma (Dahl et al. 1986; Walaas and Kindblom 1990, 1991; Walaas et al. 1990; Willen 1997).

1.4.3 Biopsy

Today "closed" transcutaneous, core needle biopsy techniques are widely used, often assisted by radiographic imaging techniques. Material can be obtained from both soft tissue components (preferable when possible) and intraosseous components, and the material obtained is usually sufficient for adjunctive studies such as immunohistochemistry and cytogenetic/molecular genetic analyses. If RNA-based molecular analyses are to be carried out it is important that decalcification processes if required are adjusted to allow such techniques (formic acid can be used, not nitric acid!) (Mangham et al. 2006). When for various reasons "closed" biopsy techniques cannot provide material sufficient for a definite diagnosis an open surgical biopsy has to be performed. It is important that decalcification techniques are not routinely applied on all bone lesion specimens since many specimens need no decalcification at all or at least parts of the biopsy can be processed without such procedures. The decalcification procedure has also to be adjusted for each specimen in order not to overdecalcify the tissue, which can severely hamper the possibilities to reach a correct diagnosis.

1.4.4 Curettage

A bone lesion can be curetted as a one-step diagnostic and treatment procedure or as definite treatment after previous biopsy. Generous sampling for microscopic examination is essential and the same principles for decalcification procedures should be applied as for biopsies.

1.4.5 Resections and Amputations

Resections and amputations are performed as part of curative definite treatment of bone tumors. For a correct approach to dissection of such specimens it is important that the pathologist can review pertinent radiographic images and that that the surgeon has indicated orientation if necessary. In addition to a correct histopathologic diagnosis, the examination of such specimens should include assessment of tumor size (three dimensions), margins (tissue type and dimensions), involvement of the marrow, cortex, periosteum, joints, surrounding soft tissues, etc., and possible vascular invasion. If preoperative treatment has been given, the response should be assessed based on a detailed mapping of the tumor.

1.5 Adjunctive Diagnostic Techniques

1.5.1 Histochemistry, Immunohistochemistry, and Electron Microscopy

These techniques have helped to better define many bone tumors but are, with some important exceptions, not required in routine diagnosis. For the vast majority of bone tumors the diagnosis is based on the histologic appearance in routine-stained sections with appropriate consideration of clinical setting and imaging findings. Immunohistochemical characterization, however, is of special importance for classification of metastatic bone disease (identification of primary sites if unknown) and for the subclassification of lymphohematologic malignancies and small round cell malignancies, in particular Ewing's sarcoma. Other examples where immunohistochemical findings may be helpful include the diagnosis of chordoma in biopsies, the recognition of endothelial differentiation in poorly differentiated angiosarcomas, and for the distinction between osteofibrous dysplasia (OFD) and OFD-like adamantinoma.

1.5.2 Cytogenetic/Molecular Genetic Techniques

Genetic characterization of various bone tumors has helped to better understand their nature and the pathogenetic mechanisms involved and has also given additional support for the morphology-based classifications. Examples of this include the identification of the role of the EXT 1 and 2 genes in the development of osteochondroma, osteochondromatosis, and secondary chondrosarcomas (Bovée et al. 1999). Another example is the identification of the CDH11-USP6 fusion gene caused by a 16; 17 translocation in aneurysmal bone cysts, suggesting that these lesions are probably of neoplastic nature (Oliveira et al. 2004). Other genetic findings have also made the distinction between what in the past were considered non-neoplastic, developmental disorders, such as fibrous dysplasia and Paget's disease, and true neoplasia less clear. There are even some genetic observations suggesting that synovial chondromatosis and pigmented villonodular synovitis may represent neoplastic conditions (Fletcher et al. 2002).

In a few instances karyotyping and molecular genetic techniques (such as FISH and RT-PCR techniques) have provided highly valuable diagnostic tools. The most striking example is the identification of the Ewing's sarcoma-specific translocation between the long arms of chromosomes 11 and 22 involving a fusion of the EWS gene (or rarely the FUS gene) with various other genes of the ETS transcription factor family; mostly these translocations involve the FLI1 gene, less frequently the ERG, ETV1, E1A-F, FEV or ZSG genes. FISH- and/or RT-PCR-based techniques, designed to identify these gene translocations, are today widely applied in the routine diagnosis of Ewing's sarcoma and its distinction from other small round cell malignancies (Fletcher et al. 2002; Mangham et al. 2006; Unni et al. 2005).

1.6 Classification of Bone Tumors

The histologic classification of bone tumors is based on cytologic findings (in particular cell type such as osteocyte/osteoblast, chondrocyte/chondroblast, osteoclast, etc.), architecture, and type of matrix produced by the tumor. Despite the rarity of bone tumors there is a very wide spectrum of entities with sometimes overlapping features; the current WHO classification (2002) includes a total of 45 main bone tumor types. For some malignant bone tumors, such as osteosarcoma and chondrosarcoma, malignancy grading is important, while for others such as Ewing's sarcoma and chordoma the degree of malignancy is implicated in the diagnosis. In addition to correct classification and in some cases grading, the pathologist has to report on margins, relation of tumor to cortex, periosteum, surrounding soft tissues, joints, etc., and the presence of vascular invasion as well as give information of importance for staging (Dorfman and Czerniak 1998).

The current classifications of benign and malignant bone tumors are summarized in Tables 1.2 and 1.3 and the most common non-neoplastic bone tumor-simulating conditions in Table 1.4.

1.7 Comments on the Morphologic Classification of Bone Tumors

1.7.1 Cartilage Tumors

The morphologic diagnosis of cartilage tumors poses particular problems. The distinction between benign cartilage lesions and chondrosarcoma is tradition-

Table 1.4. Classification of most common conditions simulating primary bone tumors, peak age, and common sites

Histologic type	Peak age (years)	Most common sites	Comments
Aneurysmal bone cyst	5–20	Femur, tibia, humerus, vertebrae	Metaphyseal in long bones
Simple bone cyst	Infancy to 20	In childhood: proximal femur, humerus and tibia In adults: calcaneus, ilium	
Fibrous dysplasia	5–30	Long bones, jaws, skull, ribs	One third polyostotic Rarely combined with endocrine disorders
Non-ossifying fibroma	5–20	Distal femur, proximal and distal tibia	Synonym: metaphyseal fibrous (cortical) defect
Osteofibrous dysplasia	Infancy to 20	Tibia	Diaphyseal Rarely in fibula, ulna, radius
Langerhans cell histiocytosis	Infancy to 30	Skull, femur, pelvis, mandible	May be polyostotic Very rarely disseminated disease, visceral involvement
Pigmented villonodular synovitis	10–40	Localized: fingers Diffuse: knee, hip, ankle	Synonym for localized: GCT of tendon sheath Diffuse: may destroy bone
Synovial chondromatosis	20–40	Knee, hip	May erode bone Chondrosarcoma may involve synovium and simulate synovial chondromatosis
Paget's disease	50–90	Pelvis, craniofacial bones, spine, femur, tibia	Sporadic cases may develop secondary high-grade sarcoma (1%) Familial cases may present at young age

GCT giant cell tumor

ally stated to be based on cellularity, degree of atypia, myxoid stromal change, and growth characteristics in relation to native bone. However, the vast majority of chondrosarcomas are low grade and very highly differentiated with minimal atypia and the identification of permeating, infiltrative growth in native bone may not be possible to find in biopsies. Moreover, several types of benign cartilage lesions may show overlapping morphology with chondrosarcoma by being fairly cellular and showing myxoid change and variation in cell size and shape. Periosteal chondroma, enchondroma of phalanxes, soft tissue chondroma, and synovial chondromatosis as well as enchondromas in the setting of Ollier's disease and Maffucci's syndrome are such examples. The interobserver variability in distinguishing benign cartilage lesions from chondrosarcomas and grade 1 chondrosarcomas from grade 2 tumors has been found to be remarkably poor even among specialized bone tumor pathologists (Eefting et al. 2008). This fact underscores the importance of integrating clinical setting and imaging findings in all diagnoses of cartilage lesions. Even when all clinical, imaging, and morphologic information is considered, a significant number of cartilage lesions remains of uncertain malignant potential (so-called CLUMPs). CLUMP has therefore become a useful concept when dealing with intraosseous well-differentiated cartilage tumors without obvious malignant features histologically but of significant size (> 5 cm).

1.7.2 Bone-forming Tumors

The distinction between osteoid osteoma and osteoblastoma is primarily based on clinical setting and imaging findings since they have very similar or identical histologic characteristics. A subset of osteoblastomas is characterized by unusually large epithelioid osteoblasts, larger tumor size, and occurrence in an older age group. The term aggressive osteoblastoma has been suggested for these since they have been reported to recur and cause clinical problems more frequently than the classic ones (Dorfman and Weiss 1984). This finding remains controversial, however.

The most important and sometimes problematic distinction is of course between osteoblastoma and osteosarcoma. The diagnosis of osteosarcoma is usually fairly uncomplicated, the vast majority being high grade of either osteoblastic, chondroblastic, or fibroblastic types. Diagnostic problems typically occur when osteosarcomas occur at unusual sites and in unusual age groups or have unusual morphologic features. Moreover, osteoblastoma-, chondroblastoma-, and chondromyxoid fibroma-like variants of osteosarcoma do occur. A telangiectatic osteosarcoma may in a biopsy show areas that with difficulty can be distinguished from an aneurysmal bone cysts and giant cell-rich osteosarcomas may focally closely mimic giant cell tumors. The very rare small cell variant of osteosarcoma may show features overlapping with Ewing's sarcoma.

The very low grade osteosarcomas may also pose difficulties for the pathologist. Parosteal osteosarcoma may show features overlapping with heterotopic ossification and when presenting a "cartilage cap" with osteochondroma. The low-grade central osteosarcomas may be difficult to distinguish from fibrous dysplasia and desmoplastic fibroma (Dorfman and Czerniak 1998; Unni et al. 2005).

1.7.3 Ewing's Sarcoma and Other Small Round Cell Malignancies

The vast majority of primary small round cell malignancies occurring in bone are within the family of Ewing's sarcomas. Primitive neuroectodermal tumor (PNET) is a term sometimes used for the subset with distinctive neuroectodermal features as seen light microscopically, ultrastructurally, or immunohistochemically. In biopsy material, the distinction from malignant lymphoma is the most important. Immunohistochemical findings (positive for CD99 but negative for lymphocytic markers) and genetic/molecular genetic characteristics (11;22 translocation and identification of typical fusion transcripts) help to recognize the Ewing's sarcomas (Dorfman and Czerniak 1998; Mangham et al. 2006; Unni et al. 2005).

Rarely other small round cell malignancies enter the differential diagnoses, such as metastatic neuroblastoma, primary rhabdomyosarcoma of bone, and the rare small cell variant of osteosarcoma (Dorfman and Czerniak 1998; Unni et al. 2005).

1.7.4 Giant Cell Tumors

The morphologic characteristics of giant cell tumor of bone, combined with the striking consistency in age and site distribution make the diagnosis fairly straightforward in most instances. Sometimes, however, giant cell tumors present unusual features that may cause problems, such as extensive spindle cell areas, prominent new bone formation, rarely cartilage formation, secondary aneurysmal bone cyst development, and nuclear enlargement and hyperchromasia. Moreover, a number of other bone lesions are also characterized by numerous osteoclast-type giant cells, such as chondroblastoma (also an epiphyseal lesion), solid variants of aneurysmal bone cysts, non-ossifying fibroma, and, not least, brown tumor associated with hyperparathyroidism. Metaphyseal location and obvious anaplasia help to recognize the giant cell-rich osteosarcomas.

A very small percentage (probably less than 3%) of histologically benign giant cell tumors metastasizes, particularly to lungs. Such metastases may follow a protracted indolent course or may be progressive and lead to the patient's death. A high-grade sarcoma component may occur de novo in giant cell tumors (primary malignant giant cell tumor or dedifferentiated giant cell tumor) or in recurrent giant cell tumors or at sites previously affected by giant cell tumors (secondary malignant giant cell tumor) (Meis 1991; Meis et al. 1989). Many of the reported secondary malignant giant cell tumors have received radiotherapy as part of their original treatment.

1.7.5 Fibrogenic/ Fibrohistiocytic Tumors

Desmoplastic fibroma, defined as a benign but locally aggressive lesion with histologic resemblance to des-

moid-type fibromatosis of soft tissues, is a rarely used concept. Its distinction from low-grade central osteosarcoma and low-grade fibrosarcoma may be problematic (Unni et al. 2005).

Fibrosarcoma is a term used for malignant spindle cell tumors with a distinct fascicular pattern and lacking osteoid or mineralized bone production (Bertoni et al. 1984). Low-grade fibrosarcomas may be difficult to distinguish from desmoplastic fibromas and high-grade fibrosarcomas from fibroblastic osteosarcomas which in biopsies may lack obvious bone matrix production. Also the distinction from malignant fibrous histiocytoma is often arbitrary and may depend on sampling.

Benign fibrous histiocytoma of bone is a term sometimes used for lesions histologically indistinguishable from non-ossifying fibroma but with a different clinical setting (usually older patients and non-metaphyseal locations).

Malignant fibrous histiocytoma remains a somewhat controversial term used for high-grade spindle cell and pleomorphic bone sarcomas lacking bone matrix production (Dahlin et al. 1977). The distinction from osteosarcomas with minimal osteoid/bone matrix production may be difficult. Malignant fibrous histiocytoma tend to occur in an older age group than osteosarcomas, peak after 40 years, and about one third of reported cases have occurred after radiotherapy or are associated with Paget's disease (Dorfman and Czerniak 1998; Unni et al. 2005).

1.7.6 Chordoma

The characteristic histologic and immunohistochemical features and site distribution of chordoma usually make the diagnosis fairly uncomplicated. In cases in which the microscopy and immunoprofile overlap with metastatic carcinoma, detection of the newly reported chordoma marker brachyury, a regulator of notochordal development, may be helpful (Vujovic et al. 2006). So-called chondroid chordoma is a rare variant occurring in the skull base, presenting classic chordoma features as well as chondroid components (Rosenberg et al. 1994). Rarely chordomas may undergo dedifferentiation to high-grade sarcomas (Bergh et al. 2000; Meis 1991). Very rare examples of chordoma have been reported in bone or soft tissues outside the midline, so-called chordoma peripheric (Tirabosco et al. 2008).

1.7.7 Vascular Tumors

Classic hemangiomas of capillary or cavernous types are common in the spine (Dorfman et al. 1971). Many of these are multicentric and often incidental findings. Other rare benign vascular lesions include epithelioid hemangioma (O'Connell et al. 1993), various types of angiomatosis, lymphangioma(tosis), and glomus tumors (Dorfman and Czerniak 1998; Unni et al. 2005).

Epithelioid hemangioendothelioma of bone is a skeletal counterpart to the same entity in soft tissues and visceral organs. They are viewed as borderline or low-grade lesions that frequently affect multiple sites (Tsuneyoshi et al. 1986). In overtly malignant cases the distinction from epithelioid angiosarcomas becomes arbitrary.

Angiosarcomas of bone show a range of differentiation and atypia from low-grade lesions with obvious vascular differentiation to predominantly solid, poorly differentiated sarcomas for which immunotechniques to demonstrate endothelial markers may be required to support the diagnosis. Practically any bone can be affected but most cases are seen in the axial skeleton and pelvic bones. When angiosarcomas affect multiple sites they are often confined to one anatomic area, such as an extremity (Dorfman et al. 1971; Unni et al. 2005).

1.7.8 Soft Tissue Tumor Types Occurring as Primary Bone Tumors

Rarely both benign and malignant tumors, typically occurring in soft tissues, present as primary bone tumors. Among such benign tumors are intraosseous lipomas (Milgram 1988), schwannomas, and leiomyomas (Fletcher et al. 2002; Unni et al. 2005). Among the malignant ones leiomyosarcoma is the most common (Berlin et al. 1987). Very rarely liposarcoma, synovial sarcoma, malignant peripheral nerve sheath tumor, clear cell sarcoma of tendons and aponeurosis, rhabdomyosarcoma, and alveolar soft part sarcoma may be primary in bone (Dorfman and Czerniak 1998; Unni et al. 2005).

1.7.9 Conditions Simulating Primary Bone Tumors

In the elderly, metastatic disease is by far the most common condition simulating primary bone tumors. Practically, the distinction becomes particularly problematic

when presenting as a solitary lesion without previous history of malignancy. Almost any type of cancer can metastasize to the skeleton but, in particular, cancer of breast, prostate, thyroid, lung, and kidney tend to metastasize to bone (Unni et al. 2005). Renal cell carcinoma is by far the most common cancer associated with solitary bone metastases.

In addition to the bone tumor-simulating conditions summarized in Table 1.4, there are a number of other lesions that may cause diagnostic problems. These include cysts, such as intraosseous ganglion cysts and epidermal inclusion cysts, and bone and cartilage-forming lesions, such as heterotopic ossification, subungual exostosis, bizarre parosteal osteochondromatous proliferation, and fracture callus. Giant cell-rich lesions that may simulate giant cell tumor of bone include so-called giant cell reparative granuloma of jaws and small bones of the hands and feet as well as "brown tumors" associated with hyperparathyroidism (Dorfman and Czerniak 1998; Unni et al. 2005).

Characteristic morphologic aspects of bone tumor diagnosis are illustrated in Figs. 1.1–1.3.

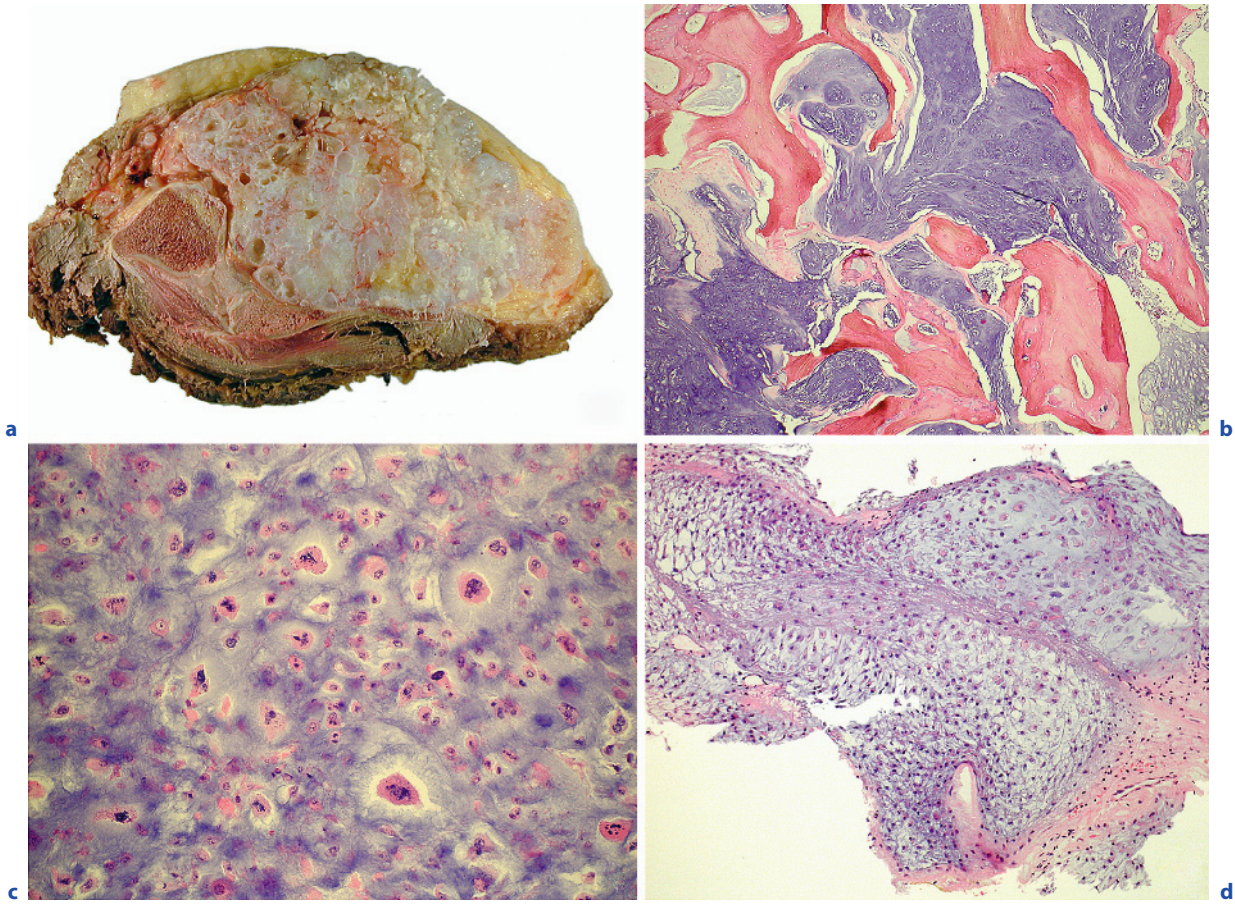

Fig. 1.1. a Pelvic resection for a large chondrosarcoma. **b** Well-differentiated chondrosarcoma with diffuse permeating growth between the bony lamellae. **c** High-grade chondrosarcoma showing prominent cytologic atypia and atypical mitotic figures. **d** Biopsy from enchondroma of a distal phalanx. Increased cellularity and myxoid change can make the distinction from chondrosarcoma difficult if clinical setting and imaging findings are not considered in the final diagnosis

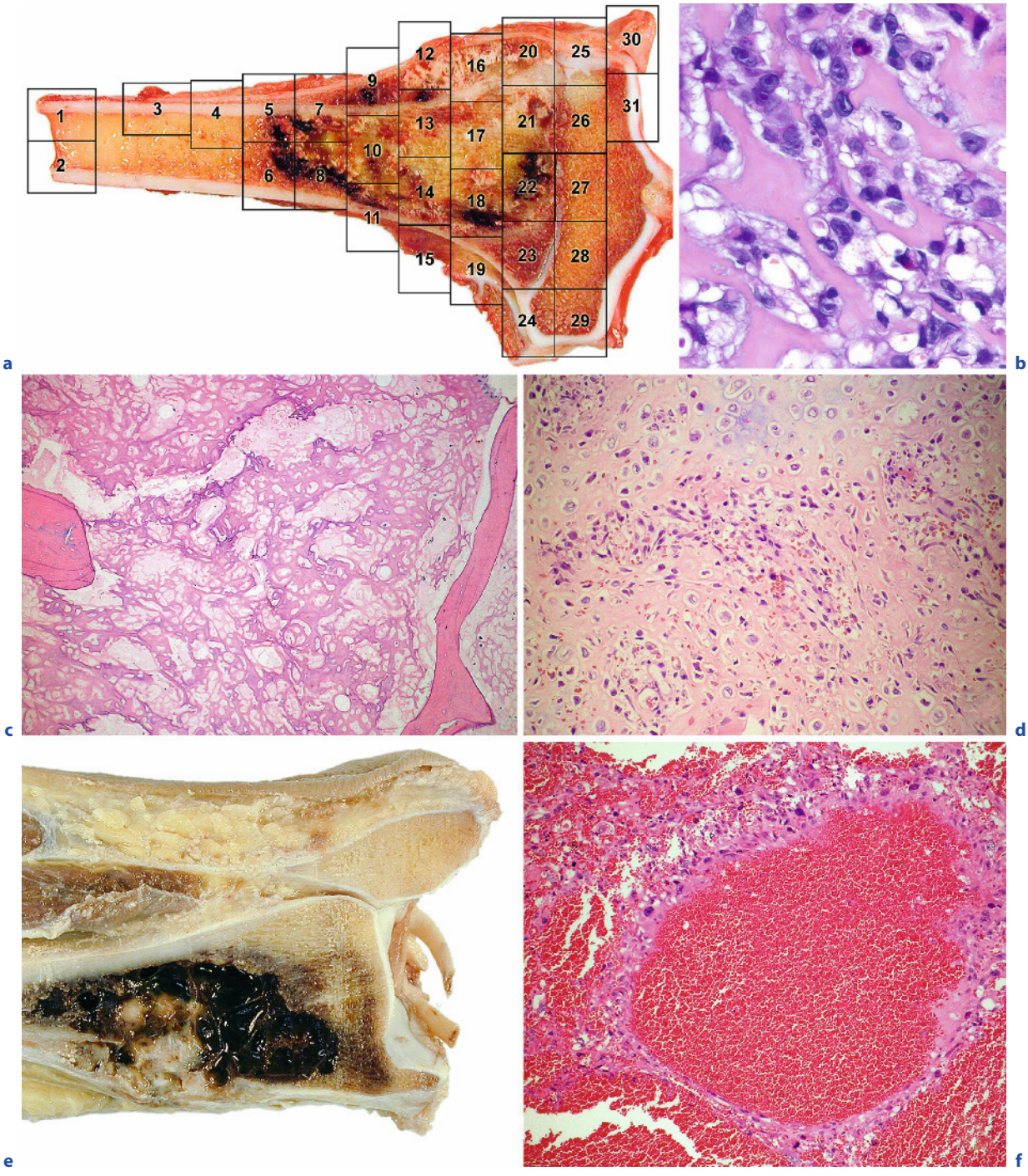

Fig. 1.2. **a** Resection of proximal tibia with typical features of osteosarcoma. Mapping of the specimen is done in order to evaluate the response to given preoperative chemotherapy. **b** Pretreatment biopsy of high-grade osteoblastic osteosarcoma. **c** After treatment the tumor is replaced by a network of acellular mineralized bone indicating good response. **d** Active fracture callus may show features resembling osteosarcoma but lack true anaplasia. **e** Resection of lower leg showing a telangiectatic osteosarcoma in the distal tibia. **f** Telangiectatic osteosarcoma resembles an aneurysmal bone cyst but shows severe cytologic atypia

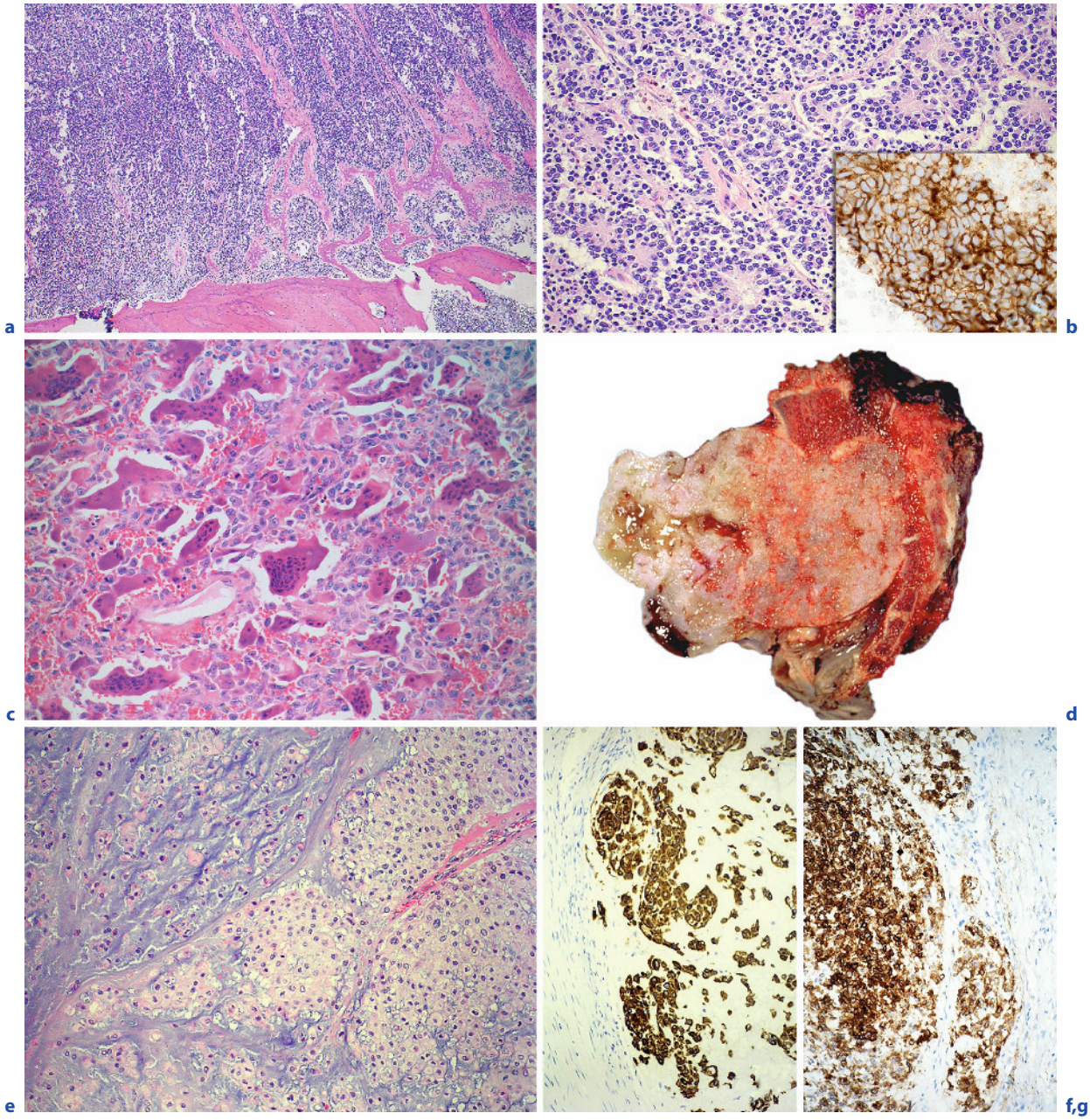

Fig. 1.3. **a,b** Ewing's sarcoma showing a diffuse proliferation of small primitive cells, focally with rosette-like formations (**b**). *Inset* in **b** is immunohistochemical demonstration of CD99. **c** Giant cell tumor of bone showing very large osteoclasts in a mononuclear cell background. **d** Total resection of sacrum with a large chordoma. **e** Chordomas resemble notochordal tissue and are characterized by epithelioid tumor cells in sheaths and strands, enclosed by an abundant myxoid matrix. **f,g** Chordomas show epithelial features immunohistochemically, thus positivity for cytokeratin (**f**) and epithelial membrane antigen (**g**)

Table 1.5. Syndromes associated with bone tumors

Syndrome	Manifestations
Bloom syndrome	AR; growth deficiency, immunodeficiency, early development of cancer including osteosarcoma
Familial expansile osteolysis	AD; osteosarcoma
Langer-Giedion syndrome	Sporadic; combination of tricho-rhino-phalangeal syndrome II and multiple osteochondromas; chondrosarcomas
Li-Fraumeni syndrome	AD; early onset of various malignancies including osteosarcomas and soft tissue sarcomas
Maffucci's syndrome	Sporadic; multiple enchondromas, chondrosarcoma, hemangioma, spindle cell hemangioma, angiosarcoma
Ollier's disease	Sporadic; multiple enchondromas
Multiple osteochondromas (osteochondromatosis)	AD; multiple osteochondromas, secondary chondrosarcoma, very rarely osteosarcoma
Mazabraud syndrome	Sporadic; polyostotic fibrous dysplasia, osteosarcoma, intramuscular myxoma
McCune-Albright syndrome	Sporadic; polyostotic fibrous dysplasia, osteosarcoma, endocrine disorders, skin pigmentation
Familial Paget's disease	AD; early onset Paget's, osteosarcoma
Retinoblastoma	AD; osteosarcoma, soft tissue sarcomas
Rothmund-Thomson syndrome	AR; poikiloderma, sparse hair, small stature, skeletal abnormalities, increased risk of cancer including osteosarcoma
Werner's syndrome	AR; premature aging, increased risk of various bone and soft tissue sarcomas

AD autosomal dominant, *AR* autosomal recessive

1.8 Congenital, Hereditary, and Non-hereditary Syndromes Associated with Bone Tumors

There are a large number of hereditary and non-hereditary conditions and syndromes associated with an increased risk of developing bone tumors. For many of these the genetic background has recently been clarified giving important knowledge of the pathogenetic mechanisms involved. Table 1.5 summarizes the most important of these conditions (Fletcher et al. 2002).

References

Bergh P, Kindblom LG, Gunterberg B, et al. (2000) Prognostic factors in chordoma of the sacrum and mobile spine: a study of 39 patients. Cancer 88:2122–2134

Berlin O, Angervall L, Kindblom LG, et al. (1987) Primary leiomyosarcoma of bone. A clinical, radiographic, pathologic-anatomic and prognostic study of 16 cases. Skeletal Radiol 16:364–376

Bertoni F, Capanna R, Calderoni P, et al. (1984) Primary central (medullary) fibrosarcoma of bone. Semin Diagn Pathol 1:185–198

Bovée JV, Cleton-Jansen AM, Wuyts W, et al. (1999) EXT-mutation analysis and loss of heterozygosity in sporadic and hereditary osteochondromas and secondary chondrosarcomas. Am J Hum Genet 65:689–698

Dahl I, Akerman M, Angervall L (1986) Ewing's sarcoma of bone. A correlative cytological and histological study of 14 cases. Acta Pathol Microbiol Immunol Scand (A) 94:363–369

Dahlin DC, Unni KK, Matsuno T (1977) Malignant (fibrous) histiocytoma of bone: fact or fancy? Cancer 39:1508–1516

Dorfman HD, Czerniak B (1995) Bone cancers. Cancer 75:203–210

Dorfman HD, Czerniak B (1998) Bone tumors. Mosby, St Louis

Dorfman HD, Weiss SW (1984) Borderline osteoblastic tumors: problems in the differential diagnosis of aggressive osteoblastoma and low grade osteosarcoma. Semin Diagn Pathol 1:215–234

Dorfman HD, Steiner GC, Jaffe HL (1971) Vascular tumors of bone. Hum Pathol 2:349–376

Eefting D, et al. (2008) Assessment of interobserver variability and histological parameters to improve reliability in classification and grading of central cartilaginous tumors. Am J Surg Pathol (in press)

Fletcher CDM, Unni KK, Mertens F (eds) (2002) Pathology and genetics of tumours of soft tissue and bone. WHO classification of tumours. IARC Press, Lyon

Mangham DC, Williams A, McMullan DJ, et al. (2006) Ewing's sarcoma of bone: detection of specific transcripts in a large consecutive series of formalin-fixed decalcified paraffin-embedded tissue samples using the reverse transcriptase-polymerase chain reaction. Histopathology 48:363–376

Meis JM (1991) "Dedifferentiation" in bone and soft-tissue tumors. A histological indicator of tumor progression Pathol Annu 26:37–62

Meis JM, Dorfman HD, Nathanson SD, et al. (1989) Primary malignant giant cell tumor of bone: "dedifferentiated" giant cell tumor. Mod Pathol 2:541–546

Milgram JW (1988) Intraosseous lipomas. A clinicopathologic study of 66 cases. Clin Orthop 231:277–302

O'Connell JX, Kattapuram SV, Mankin HJ, et al. (1993) Epithelioid hemangioma of bone. A tumor often mistaken for low-grade angiosarcoma or malignant hemangioendothelioma. Am J Surg Pathol 17:610–617

Oliveira AM, His BL, Weremowicz S, et al. (2004) USP6 (Tre2) fusion oncogenes in aneurysmal bone cyst. Cancer Res 64:1920–1923

Rosenberg AE, Brown GA, Bhan AK, et al. (1994) Chondroid chordoma: a variant of chordoma. A morphologic and immunohistochemical study. Am J Clin Pathol 101:36–41

Tirabosco R, Mangham DC, Rosenberg AE, et al. (2008) Brachyury in extra-axial skeletal and soft tissue chordomas: a marker that distinguishes chordoma from mixed tumor/myoepithelioma/parachordoma in soft tissue. Am J Surg Pathol 32:572–580

Tsuneyoshi M, Dorfman HD, Bauer TW (1986) Epithelioid hemangioendothelioma of bone. A clinico-pathologic, ultrastructural and immunohistochemical study. Am J Surg Pathol 10:754–764

Unni KK, et al. (2005) Tumors of the bones and joints. AFIP atlas of tumor pathology, series 4. American Registry of Pathology, Washington DC

Vujovic S, Henderson S, Presneau N, et al. (2006) Brachyury, a crucial regulator of notochordal development, is a novel biomarker for chordomas. J Pathol 209:157–165

Walaas L, Kindblom LG (1990) Light and electron microscopic examination of fine-needle aspirates in the preoperative diagnosis of osteogenic tumors: a study of 21 osteosarcomas and two osteoblastomas. Diagn Cytopathol 6:27–38

Walaas L, Kindblom LG (1991) Fine-needle aspiration biopsy in the preoperative diagnosis of chordoma: a study of 17 cases with application of electron microscopy, histochemical and immunocytochemical examination. Hum Pathol 22:22–28

Walaas L, Kindblom LG, Gunterberg B, et al. (1990) Light and electron microscopic examination of fine-needle aspirates in the preoperative diagnosis of cartilaginous tumors. Diagn Cytopathol 6:396–408

Willen H (1997) Fine needle aspiration in the diagnosis of bone tumors. Acta Orthop Scand Suppl 273:47–53

Computed Tomography of Bone Tumours

2

Richard W. Whitehouse

CONTENTS

2.1 **Introduction** *17*

2.2 **Developments in Computed Tomography** *18*
2.2.1 CT Technology *18*
2.2.2 Dual-Energy Scanning *19*
2.2.3 Single Gantry Rotation Volume Scanning *19*
2.2.4 CT "Fluoroscopy" *19*
2.2.5 Data Manipulation *19*

2.3 **Scan Image Quality** *20*
2.3.1 Internal Metalwork from Fixation Devices *21*
2.3.2 CT Number, Hounsfield Units, Window Width and Levels *22*
2.3.3 Radiation Dose Reduction *23*

2.4 **CT of Bone Tumours** *24*
2.4.1 Anatomy *24*
2.4.2 Patient Positioning *24*

2.5 **Indications** *24*
2.5.1 Thoracic Staging *25*
2.5.2 Whole-Body CT Scanning *26*

2.6 **CT-Guided Interventions** *26*

2.7 **Conclusion** *28*

References *28*

KEY POINTS

- Computed tomography (CT) is a high-radiation-dose examination, which should therefore be both justified and tailored to the clinical need.
- CT of solitary bone lesions may provide information on tumour mineralization difficult to identify on plain film or MR.
- Non-contrast-enhanced CT of the thorax is appropriate for staging of metastatic bone sarcoma.
- Whole-body CT in older patients should be considered where the "index" bone lesion may be a metastasis.
- CT with CT fluoroscopy is ideal for guiding bone biopsy and interventional procedures. Steps to minimize radiation dose are important for both the patient and operator.
- Ingenuity in patient positioning can produce high-quality scans of limb lesions (by removing unnecessary parts of the patient from the scan plane).

2.1 Introduction

Although magnetic resonance (MR) imaging has become the primary imaging modality for local staging of bone tumours, computed tomography (CT) has complementary roles in the diagnosis and local staging of bone tumours, as well as operation planning, custom prosthesis production, biopsy and percutaneous treatment guidance. Scanning the chest for detection of pulmonary metastases is also a primary role for CT. Computed tomography remains essential for the assessment of patients in whom MR is contraindicated (e. g.

R. W. Whitehouse, MD
Department of Clinical Radiology, Manchester Royal Infirmary, Oxford Road, Manchester, M13 9WL, UK

due to intracranial aneurysm clips or cardiac pacemakers). By comparison with histological measurement of metastatic tumour size in resected spinal lesions, CT underestimates size, whereas MR overestimates it (Fujita et al. 2000), an observation probably also true for other tumours and in other locations.

2.2 Developments in Computed Tomography

A CT image is a map of normalized X-ray attenuation coefficients, generated by computer, from filtered back projection of X-ray transmission measurements in multiple directions through the object in question. Each pixel in the image represents the averaged attenuation of the material that occupies the corresponding voxel in the subject. Recent developments in CT include helical scanning, multislice acquisition, single rotation volume scanning, simultaneous dual-energy scanning and real-time CT "fluoroscopy" (Dawson and Lees 2001). The number of slices acquired in a single rotation of the gantry continues to increase with newer scanners able to perform a scan with over 300 sub-millimetre slices using a single gantry rotation in under 1 s.

2.2.1 CT Technology

The CT gantry carries the X-ray tube(s), X-ray detectors and associated electronics. Developments in power transfer to the X-ray tubes and data transfer from the detectors over the past three decades have increased scan data acquisition speeds from approximately one slice every 5 s in the early 1980s to several hundred slices in under a second in 2008. The speed of digital processing of the data to produce images has also improved exponentially, giving almost instant image display. The continuous supply of detector output data allows both helical scanning and CT fluoroscopy.

Shorter slice acquisition times result in a requirement for X-ray tubes to have both a higher heat capacity and a higher maximum tube current, as the mAs required for a single slice remains much the same but the time in which the slice is acquired is reduced. In addition, for helical scanning continuous X-ray output for up to 60 s may be required. High mA scans, with extended anatomical coverage, can be obtained with ease from multislice helical scanners, with consequent high radiation doses to patients.

Helical scanning is performed by moving the table continuously during the gantry rotation and X-ray exposure, from the first slice location to the last; thus, a helix of X-ray transmission data through the scan volume is acquired. To generate a CT image the data from adjacent turns of the helix are interpolated to produce transmission data which are effectively from a single slice location (Kalender et al. 1990). This process can be performed at any location within the helix (except the first and last 180° – where there is no adjacent helix of data for interpolation). In this way overlapping slices can be produced without overlapping irradiation to the patient. The relationship between the X-ray fan-beam collimation and the table movement per rotation of the gantry is called the pitch ratio. Extended or stretched pitch scans are performed with pitch ratios greater than 1. Such extended pitches can be used to trade off between greater scan volumes, shorter scan acquisition times and lower scan radiation doses. Stretching the pitch ratio to 1.25 has little effect on the image appearances, but pitch ratios greater than 1.5 produce images with effective slice thickness, significantly greater than the nominal fan-beam collimation thickness. Multislice scanners in particular may use pitch ratios of less than 1. This increases patient radiation dose and scan acquisition time but reduces image noise and some spiral scanner artefacts. By increasing the number of detector arrays ("multislice scanner") several interlaced helices can be acquired simultaneously with the table increment per gantry rotation increased proportionately (McCollough and Zink 1999). Initial developments in multislice scanners were aimed at reducing individual slice thicknesses, but once z-axis resolution is equivalent to in-plane resolution, further reduction in slice thickness is of limited value. Adding further rows of detectors will then increase the total width of the detector bank. While offering the potential for faster scan acquisition, the increasing divergence of the X-ray beam to the outer rows of detectors creates a "cone-beam" geometry for the X-ray-beam paths, requiring complex data corrections to reduce artefacts in the resultant images. Currently, scanners offering up to 320 detector rows with up to 16 cm total detector width are available. Flat-panel detectors, based on the Direct Digital Radiography technology, for CT data acquisition are under development. These detectors will allow higher resolution, increased total detector width and variable effective slice thickness (Obenauer et al. 2007). The result of these developments will be a scanner that can acquire the full examination data from a single gantry rotation without table movement. Although this offers significant reduction in acquisition time and total X-ray tube loading, radiation dose reduction techniques

that modulate the X-ray tube current according to slice location will no longer be applicable.

Currently available individual detector widths of between 0.5 and 0.75 mm can achieve y-axis resolution equivalent to in-plane resolution, giving true isometric voxels and consequent equivalent quality reformats in any plane. Even with the thinnest detector widths, the best y-axis resolution is achieved from overlapping sections reconstructed at the thinnest available slice width and reconstructed at half-slice-width spacing (or less).

The combination of multislice and helical scanning results in volume scan acquisition times which are many times faster than a single-slice helical scanner with the same gantry rotation speed, and one or even two orders of magnitude faster than a non-spiral scanner. Multislice scanning reduces X-ray tube loading requirements as the scanner acquires several slices simultaneously with the same tube loading as a single slice would require. The patient radiation dose, however, is not directly reduced and may be increased if greater volumes are scanned.

2.2.2 Dual-Energy Scanning

Although dual-energy CT scanning has been performed by repeating scans after changing the tube voltage, the time delay between these two acquisitions results in misregistration of data from the two acquisitions due to patient movement. A helical scanner with two X-ray tubes set at different kVp levels in the same gantry allows almost simultaneous acquisition of dual-energy X-ray attenuation data. From these data separate CT images of soft tissue (bone) mineral and contrast media can be generated. The use of this scanner in assessment of bone tumours has not been evaluated; it may offer higher sensitivity and specificity to the presence of mineralization in tumours and may also increase sensitivity to contrast enhancement.

2.2.3 Single Gantry Rotation Volume Scanning

With increasing detector row numbers and coverage, true volume scanning becomes possible without requiring the table movement that is used to give a helical acquisition. A single, sub-second gantry rotation then produces hundreds of sub-millimetre-thick sections simultaneously, with a coverage of over 15 cm. The value of such scanners in the assessment of bone tumours has not yet been evaluated. Apart from increased throughput and reduced movement artefact, the potential to perform tumour perfusion studies warrants consideration.

2.2.4 CT "Fluoroscopy"

Continuous CT gantry rotation and data acquisition without table movement provides continuously updated X-ray transmission data from which revised images can be generated. With extremely rapid processors and appropriate reconstruction algorithms, further delay for image reconstruction can be minimized and a continuously updated CT image displayed in "near real time" (Hsieh 1997). Such "CT fluoroscopy" imaging can be used for CT-guided interventional procedures (De Mey et al. 2000). As with all fluoroscopic procedures care should be taken to reduce fluoroscopy time to the minimum necessary and to avoid operator irradiation – instruments designed to keep the operators hands out of the CT section (Daly et al. 1998) and use of the lowest selectable tube current are advocated (50 mA is claimed to be sufficient; Froelich et al. 1999). The present author routinely uses 10-mA tube current for CT fluoroscopy of limbs. To assist in maintaining short CT fluoroscopy exposure times, routine recording and auditing of fluoroscopy exposure times is advocated. An audible alarm after a preset exposure time may also assist in keeping exposures as short as possible. The use of a lead drape adjacent to the irradiated volume has been demonstrated to reduce operator exposure (Nawfel et al. 2000). High skin doses to patients and operators will occur if care is not taken.

2.2.5 Data Manipulation

The vast masses of imaging data acquired from a multislice spiral scanner produces problems of data storage and interpretation. With isometric voxels, reformatted images in any other image plane will have the same image quality as the acquisition images. Fast workstations, allowing rapid reformatting and display of examinations in the most appropriate plane for the pathology being demonstrated, are therefore necessary. Post-processing image reconstructions (curved planes, surface-rendered 3D images, minimum or maximum intensity projections, "transparent bone") can also be applied to assist in diagnosis or treatment (Figs. 2.1, 2.2).

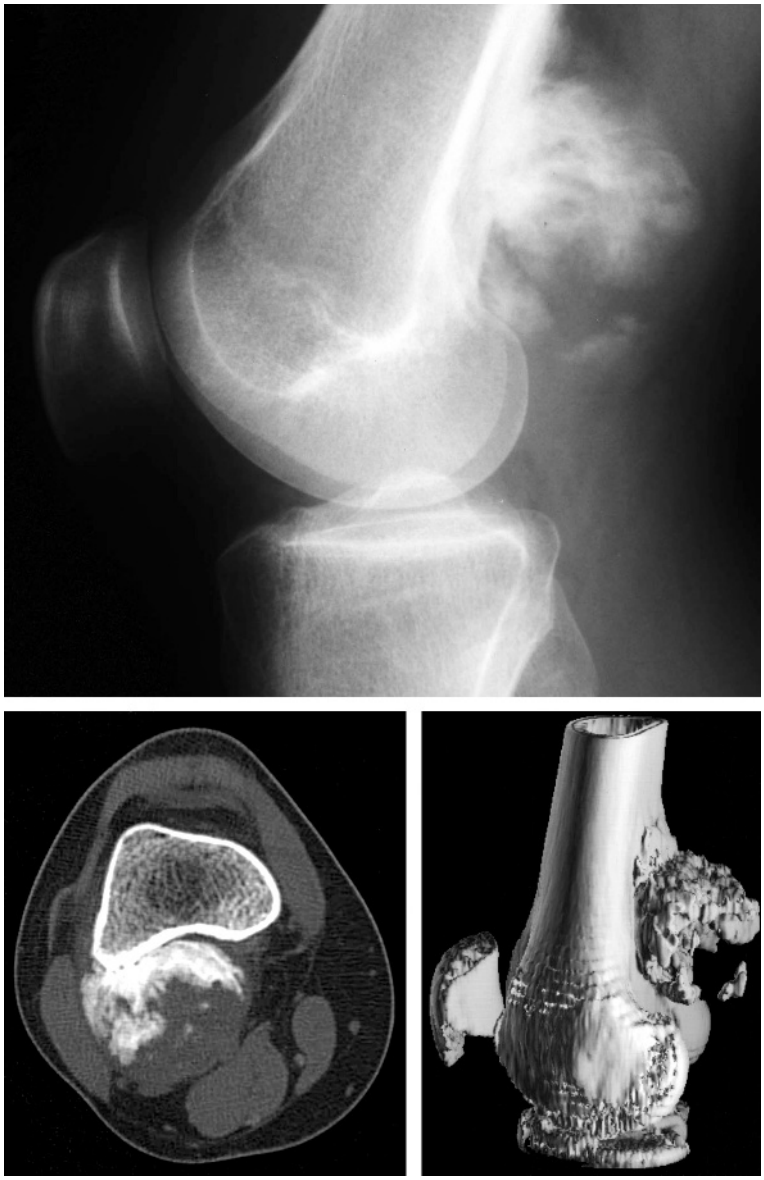

Fig. 2.1. Plain film (**a**), axial CT (**b**) and (**c**) surface reconstruction of a parosteal osteosarcoma of the distal femur. (Courtesy of A.M. Davies)

2.3 Scan Image Quality

The amount of noise, beam-hardening and streak artefacts in a CT image are dependent upon the following factors:

1. Collimation slice thickness
2. Partial or full rotation data set
3. Mass and distribution of tissue in the scan plane
4. Scan acquisition time/patient movement
5. High-density extraneous material (e.g. contrast medium spills, surgical metalwork)
6. KVp and mAs
7. Field of view
8. Matrix size
9. Reconstruction algorithm
10. Post-processing image sharpening or softening filters
11. Viewing window width and level settings

Most of these factors are amenable to selection or modification by the scanner operator and can markedly affect the quality of the final image. The relationships between image noise, mAs and patient size are non-linear, with a halving of patient size (cross-sectional area) resulting in

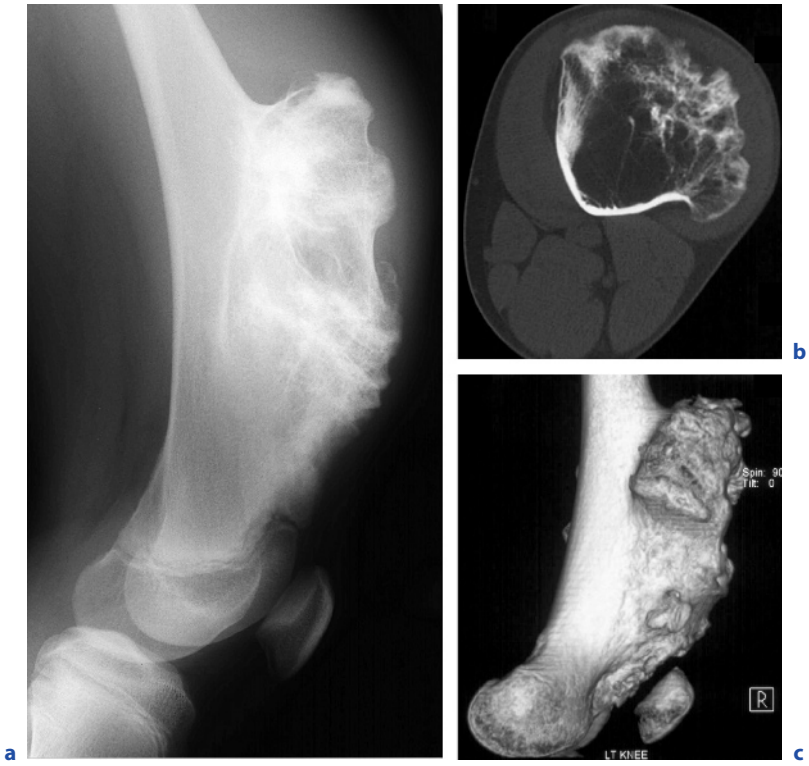

Fig. 2.2a–c. Plain film (**a**), axial CT (**b**) and (**c**) surface reconstruction of an osteochondroma of the distal femur. (Courtesy of A.M. Davies)

a quartering of image noise, whereas a fourfold increase in mAs is needed to halve the image noise. For small patients, image noise is effectively low at all mAs settings and the absolute reduction in image noise achieved by quadrupling the mAs is small.

In addition, when imaging osseous lesions, the width of the usual viewing window for bone renders noise less perceptible. As children are more radiation sensitive than adults as well as smaller, particular attention should be paid to reducing the mAs in this group of patients. Reducing the kVp also reduces patient radiation dose while also increasing the CT number difference between mineral and soft tissue. For small patients (paediatric patients in particular) this should also be considered.

Streak artefacts can be generated by high-density material within the scan plane but outside the field of view of the scanner. Tabletops, which contain edge grooves, tracks for the fixing of attachments or detachable mattresses can act as traps for spilt contrast media. Contrast droplets on the gantry window will also cause imaging artefacts. Scrupulous care to keep the tabletop and gantry clean is needed to remove these sources of artefact. Lightweight casts and plaster of paris casts do not significantly impair CT scan images of the contained limb, unless metallic components have been incorporated.

2.3.1 Internal Metalwork from Fixation Devices

The streak artefact generated from in-situ intramedullary rods is rarely excessive and does not prevent adequate assessment of the bone cortex, making CT valuable in assessing cortical bone near prostheses in selected cases. More intrusive streak artefact is seen when the CT image plane is through locking screws in intramedullary rods, bone surface plates, hip-joint replacements or fixation screws. Care in patient positioning (including decubitus positions where necessary) combined with gantry angulation in order to align the scan plane with the long axis of any screws present will reduce the number of sections degraded by streak artefact from the screws to a minimum.

In scanners with operator-selectable kVp, the use of the highest kVp setting and the use of higher mAs settings are claimed to reduce streak artefact from metalwork, although this has not been confirmed in some studies (Haramati et al. 1994; Lee et al. 2007; Link et al. 2000). The combination of increased kVp and mAs results in considerably greater tube loading and patient irradiation; consequently, the value of significantly increasing these parameters in the presence of metalwork should be considered with care. Streak artefact may appear visually less intrusive on volume-rendered (3D) images (Pretorius and Fishman 1999). The streak artefact from titanium prostheses is less than that from cobalt–chrome (Haramati et al. 1994). The use of an extended CT number scale (with a maximum window width of 40,000) may also improve the demonstration of metalwork (Link et al. 2000).

2.3.2 CT Number, Hounsfield Units, Window Width and Levels

The scale of numbers used to define the grey scale in CT images is artificially limited by data-storage constraints. The CT number scale runs from –1,000 for air, through 0 for water. The top end of the scale is usually constrained to fit into a 12-bit binary number (allowing number values from –1024 to +3072 to be stored), although extended-scale imaging with a maximum window width approximately ten times greater than this may be of value for imaging in the presence of metalwork. The Hounsfield unit (HU) is the true value which the CT number should represent. Scanner drift, calibration error, artefact or other limitation may render this inaccurate, which is why measurements made from scan images are best called CT numbers.

The Hounsfield unit value for any material is defined by Eq. 2.1:

$$HU_s = 1{,}000\ (m_s\text{-}m_w/m_w), \qquad 2.1$$

where HUs = the Hounsfield unit value for substance s, m_s = linear attenuation coefficient for substance s and m_w = linear attenuation coefficient for water.

This formula relates the HU value to the linear attenuation coefficients of the material being measured and water. As the linear attenuation coefficients of all materials change with X-ray-beam energy, there are consequently only two fixed points on the Hounsfield scale. These points are –1,000, which is the HU value for no X-ray attenuation (i.e. a vacuum), and zero, which corresponds to the HU value for water (at the calibration pressure and temperature for the scanner). The HU scale is open ended, with high-atomic-number, high-density materials having values much in excess of the upper end of the usual scale (even on "extended-scale" scanners).

The theoretical Hounsfield value for dense cortical bone calculated at an effective beam energy of 65 keV (equivalent to a scanner operating at around 120 kVp) is in the region of 1,600 (Fig. 2.3). At lower energies (e.g. 55 KeV – the approximate effective energy of a scanner operating at 80 kVp), the HU value for dense cortical bone is over 2,000. Other high-atomic-number materials (contrast media, aluminium and metal fixation devices) also show marked variation in HU value with beam energy. By contrast, the HU values of soft tissues, collagen and fat vary very little with effective beam energy as the linear attenuation coefficients because these materials closely follow those of water. Consequently, in scanners which allow the operating voltage to be changed, the CT number for bone can be increased by using a low kVp (around 80 kVp). This increases the dependence of the CT number on the presence of bone or calcification.

For lower-atomic-number materials, such as are present in soft tissues, the X-ray attenuation and consequent CT number is predominantly influenced by the electron density of the material, which is, in turn, closely related to the physical density of the material. Even the CT number of water is influenced by differences in temperature and differences in density exist between water at room and body temperature (Whitehouse et al. 1993). The presence of protein or high concentrations of salts will increase the CT number of body fluids. Measurement of the CT number of a region of interest in an image must therefore be considered only a guide to its composition.

The visual impression of the density of a region of interest is influenced by the window and level settings of the image, the calibration of the display and the densities in the surrounding part of the image. Particularly within bone, the surrounding high density of bone can give a lytic lesion the visual impression of a lower density than actually exists. Consequently, measurement rather than estimation of any region of interest is essential.

The window width and level are calibrated contrast and brightness settings for image display. The most appropriate window level for cortical bone will be influenced by the bone density and the effective scan energy, whereas the window width may need to be quite narrow to demonstrate subtle intracortical density changes.